Phonon side bands in the optical emission of zinc-blende-type semiconductors

C. Trallero-Giner* and M. Cardona
Max-Planck-Institut für Festkörperforschung, Heisenbergstrasse 1, D-7000 Stuttgart 80, Federal Republic of Germany

F. Iikawa
Instituto de Física "Gleb Wataghin," Universidade Estadual de Campinas, CEP-13081, CP-6165, Campinas, São Paulo, Brazil
(Received 2 March 1993)

A model for the LO-phonon-related structure observed in the luminescence above the gap of InP is presented. The corresponding exciton-phonon quasiparticle spectrum is calculated for zinc-blende-type semiconductors using a Green's-function formalism. It is shown that resonances may appear due to the interaction of the exciton continuum with excitations involving a 1s-exciton state plus a LO phonon. The corresponding electron-hole nonequilibrium distribution function is derived by solving the master equation, which depends on the rate of scattering by acoustic and optical phonons. These results enable the evaluation of the dependence of the luminescence intensity on light frequency and temperature. Explicit calculations are presented for InP, CdTe, and GaAs. In the case of InP they reproduce rather well the experimental luminescence profile observed above the gap and its dependence on temperature. The calculations explain why a similar structure has not been observed in the luminescence spectra of GaAs and CdTe.

I. INTRODUCTION

The observation at low temperatures of a peculiar weak structure in the laser-excited photoemission of InP approximately one LO-phonon frequency above the gap was reported in Ref. 1. The typical hot luminescence tail observed in InP above the lowest gap E_0, which decreases monotonically towards higher energies, is modified by weak structure near the emitted photon energy $\hbar\omega_l = E_0 - R + \hbar\omega_{\rm LO}$, $\hbar\omega_{\rm LO}$ being the LO-phonon energy and R the binding energy of the free exciton. The observed structure reveals the following features.

(i) Its energy is well below that of the $E_0 + \Delta_0$ critical point at Γ and practically does not change with the frequency of the excited laser ω provided $\hbar\omega > E_0 - R + \hbar\omega_{\rm LO}$.

(ii) Its amplitude is about five orders of magnitude smaller than that in the excitonic region ($\hbar\omega_l \simeq E_0 - R$) independent of the laser frequency if $\hbar\omega > E_0 - R + \hbar\omega_{\rm LO}$.

(iii) The structure disappears rapidly with increasing temperature and does not appear for laser energy below $E_0 - R + \hbar\omega_{\rm LO}$. Moreover, a process induced by phonon absorption would conduce to an enhancement of the emission lines with temperature. Similar investigations on GaAs so far gave no evidence of such a LO frequency-related structure above the E_0 gap.

In Ref. 1 this new structure was assigned to radiative annihilation of a resonant quasiparticle involving the interaction of electron-hole pairs in the continuum with discrete 1s-exciton states plus a LO phonon. The idea of resonant coupling between excitonic states was introduced by Toyozawa and Hermanson[2] in order to interpret an optical-*absorption* structure seen for $\hbar\omega > E_0 - R$ in several ionic crystals.[3,4] Such absorption shows a peak at an energy $\hbar\omega \simeq E_0 - R + \hbar\omega_{\rm LO}$. It was pointed out that an exciton and an optical phonon may form a bound state which moves through the crystal if the exciton binding energy is close to that of the phonon. The corresponding imaginary part of the dielectric constant ϵ_2 was calculated in Ref. 2 for the case of the coupling of the 1s exciton plus a LO phonon with the 2s exciton. Sak[5] generalized this work to obtain the dielectric response of a system in which the 1s exciton + LO phonon couple with continuous states showing that $\epsilon_2(\omega)$ has a negative slope for $\omega = \omega_T$ with ω_T given by $\hbar\omega_T = E_0 - R + \hbar\omega_{\rm LO}$, reaching a maximum related to the exciton-phonon quasiparticle. The negative slope leads to a minimum in ϵ_2 above ω_T. The resulting phonon-related sideband in the absorption spectrum can thus be invoked to explain the experimental observations of Refs. 3 and 4.

In this paper we evaluate the emission rate of a system exhibiting the exciton LO–optical-phonon resonances. In Sec. II, the basic relations needed to calculate the luminescence intensity in terms of the emission probability of a light quantum by electron-hole pairs and the corresponding distribution function are presented. The self-energy, the energy spectrum of exciton-phonon quasiparticles, and the emission probability are also given in Sec. II. The electron-hole distribution function is evaluated versus temperature in Sec. III for the case in which the carrier relaxation is produced by interaction with acoustic and optical phonons. In Sec. IV the corresponding luminescence spectra are numerically evaluated for CdTe, GaAs, and InP and the predictions of the theory are compared with experimental data for InP. In Sec. V the main conclusions are summarized.

II. FORMULATION OF THE PROBLEM AND FUNDAMENTAL RELATIONS

We assume a cubic crystal with the conduction- (c) and valence- (v) band extrema at the center of the Bril-

louin zone and dipole-allowed direct transitions between them. The electron-hole spectrum will be assumed to be modified by a weak interaction with the longitudinal optical phonons. The rate at which photon emission occurs is given by[6]

$$I_{\rm em}(\hbar\omega_l) = \sum_{\mathbf{k}_e,\mathbf{k}_h} P(\mathbf{k}_e,\mathbf{k}_h)\, W_{cv}(\mathbf{k}_e,\mathbf{k}_h;\hbar\omega_l)\,, \qquad (1)$$

where $P(\mathbf{k}_e,\mathbf{k}_h)$ is the electron-hole pair (EHP) distribution function (in principle including correlation and the phonon renormalization described below), linear in the incident light intensity, $W_{cv}(\mathbf{k}_e,\mathbf{k}_h;\hbar\omega_l)$ is the probability of EHP annihilation with photon emission, $\mathbf{k}_e$ ($\mathbf{k}_h$) the electron (hole) wave vector, and ω_l is the frequency of the emitted photon. For parabolic isotropic bands the correlated electron-hole pair energy $E_{\rm ex}$ becomes

$$E_{\rm ex} = E_0 + \frac{\hbar^2K^2}{2m_T} + \Delta E, \qquad (2)$$

where $\mathbf{K} = \mathbf{k}_e + \mathbf{k}_h$ is the electron-hole pair center of the mass wave vector, $\Delta E = -R/n^2$ represents the discrete spectrum ($n = 1, 2, ...$) for $E_{\rm ex} < E_0 + \frac{\hbar^2K^2}{2m_T}$, and $\Delta E = \hbar^2k_0^2/2\mu$ is the continuum for $E_{\rm ex} \geq E_0 + \frac{\hbar^2K^2}{2m_T}$, $m_T = m_e + m_h$, $\mu^{-1} = m_e^{-1} + m_h^{-1}$, m_e (m_h) is the electron (hole) effective mass, and $\mathbf{k}_0$ corresponds to the relative wave vector of the EHP.

A. Emission probability

Using a perturbative approach the annihilation probability W_{cv} can be expressed by[1]

$$W_{cv} = \frac{2}{\hbar}{\rm Im}|\langle\hbar\omega_l\,|H_R^+|\,\mathbf{k}_e,\mathbf{k}_h\rangle|^2 G(\mathbf{k}_e,\mathbf{k}_h;\hbar\omega_l)\,, \qquad (3)$$

where H_R^+ is the crystal-photon interaction Hamiltonian and $G(\mathbf{k}_e,\mathbf{k}_h;\hbar\omega_l)$ is the electron-hole pair Green's function. For allowed direct transitions $\mathbf{K} = \mathbf{k}_e + \mathbf{k}_h \simeq 0$ and electron-hole states with energies above E_0, the matrix element $\langle\hbar\omega_l\,|H_R^+|\,\mathbf{k}_e,\mathbf{k}_h\rangle$ can be expressed as[7]

$$\langle\hbar\omega_l\,|H_R^+|\,\mathbf{k}_e,\mathbf{k}_h\rangle = \delta_{\mathbf{k}_e+\mathbf{k}_h,0}\frac{|e|}{m_0}\left(\frac{2\pi\hbar}{\omega_l n}\right)^{1/2}\hat{\epsilon}\cdot\mathbf{p}_{cv}^{\,*}\frac{e^{\pi/2k_0a}}{\sqrt{V_0}}\,|\Gamma(1+i/k_0a)|\,, \qquad (4)$$

where $\mathbf{p}_{cv}^{\,*}$ is the momentum matrix element between the valence band v and the conduction band c at $\mathbf{k} = \mathbf{0}$, n is the refractive index, $\hat{\epsilon}$ is the polarization of the photon field, e and m_0 are the electronic charge and bare electron mass, respectively, a is the exciton Bohr radius, V_0 is the normalization volume, and $\Gamma(z)$ is the gamma function. For direct transitions between the c and v bands the function G becomes the retarded single-particle Green's function with energy $E(0) = \hbar^2k_0^2/2\mu$.[8] Using the conventional notation, in the $(\mathbf{k}_0,t)$ representation, $G(\mathbf{k}_0,t)$ is defined as

$$G(\mathbf{k}_0,t) = i\left\langle C_{\mathbf{k}_0}(t)C_{\mathbf{k}_0}^{\dagger}(0)\right\rangle, \qquad (5)$$

$C_{\mathbf{k}_0}(t)$ being the one-particle operator in the Heisenberg representation, and $\langle\,\rangle$ denoting the average over the ground state of the system. In the zero-density approximation the Fourier transform $G(k_0,E)$ coincides with the causal Green's function and can be expressed in terms of the self-energy Σ (Ref. 9),

$$G(k_0,E) = \left[E - \frac{\hbar^2k_0^2}{2\mu} - \Sigma(E,k_0) + i\delta_0\right]^{-1}, \qquad (6)$$

where $\delta_0 > 0$ represents an adiabatic parameter. Equation (6) is the solution of the Dyson equation, shown in a diagrammatic way in Fig. 1(a) for the continuous states of the electron-hole pair.

Using Eqs. (4) and (6) we obtain from Eq. (3)

$$W_{cv} = -\frac{2e^2}{m_0^2}\left(\frac{2\pi}{V_0\omega_l n}\right)|\hat{\epsilon}\cdot\mathbf{p}_{cv}|^2\,\delta_{\mathbf{k}_e,-\mathbf{k}_h}\frac{\pi e^{\pi/k_0a}}{k_0a\sinh(1/k_0a)} \times{\rm Im}\left[E - \frac{\hbar^2k_0^2}{2\mu} - \Sigma(E,k_0) + i\delta_0\right]^{-1}. \qquad (7)$$

The above equation is isomorphic to the Kubo formula for the imaginary part of the dielectric function.[10] A similar expression to Eq. (7) was used by Sak[5] to study the phonon sidebands in the exciton absorption. In the case of the vanishing electron-phonon interaction the self-energy Σ tends to zero and from Eq. (7) the well-known absorption or emission probability for semiconductors is recovered.[6]

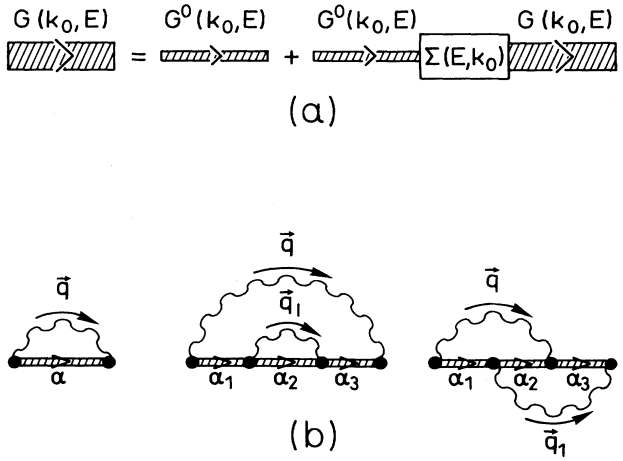

FIG. 1. (a) Diagramatic equation for the causal Green's function $G(k_0,E)$ of the electron-hole pair continuum. $\Sigma(E,k_0)$ represents the retarded self-energy due to interaction with LO phonons and $G^0(k_0,E) = [E - E(0) + i\delta_0]^{-1}$. (b) Diagrams that must be taken into account in the calculation of the self-energy Σ to various orders in the Fröhlich coupling constant.

B. Self-energy

The exciton-phonon interaction Hamiltonian is given by[11]

$$H_I = \sum_{\mathbf{q}} C_{\mathbf{q}} \left[e^{i\mathbf{q}\cdot\mathbf{r}_e} - e^{i\mathbf{q}\cdot\mathbf{r}_h} \right] b_{\mathbf{q}} + \text{H.c.}, \tag{8}$$

where $b_{\mathbf{q}}$ represents the annihilation operator for phonons with frequency ω_{LO} and wave vector $\mathbf{q}$, $\mathbf{r}_e$ ($\mathbf{r}_h$) are the electron (hole) coordinates, and $C_{\mathbf{q}}$ is the Fröhlich coupling constant for long-wavelength longitudinal phonons given by

$$C_{\mathbf{q}} = -iC_F/q\sqrt{V_0} \tag{9a}$$

with

$$C_F = \left(\frac{1}{\epsilon_\infty} - \frac{1}{\epsilon_0} \right)^{1/2} \left(2\pi\hbar\omega_{\text{LO}} e^2 \right)^{1/2}, \tag{9b}$$

ϵ_0 and ϵ_∞ being the static and the high-frequency dielectric constants, respectively.

The self-energy $\Sigma(E, k_0)$ can be obtained using standard diagrammatic techniques [Fig. 1(b)]. The resonant part of the self-energy to first order in the Fröhlich coupling constant is given by the expression

$$\Sigma(E, k_0) = \sum_{\mathbf{q},\mathbf{K}'} \sum_{\alpha} \frac{|C_{\mathbf{q}}|^2 \, |I_{\alpha,\alpha'}(\mathbf{q})|^2}{E - \Delta E_\alpha - \frac{\hbar^2 K^2}{2m_T} - \hbar\omega_{\text{LO}} + i\delta_\alpha}, \tag{10}$$

where α' represents the continuum exciton under consideration (relative wave vector $\mathbf{k}_0$, center-of-mass wave vector $\mathbf{K}' = 0$) and δ_α represents the Lorentzian width of the EHP in the intermediate state α (center-of-mass wave vector $\mathbf{K}$) which removes the nonphysical divergence at $E = \Delta E_\alpha + \hbar\omega_{\text{LO}} + \frac{\hbar^2}{2m_T} K^2$. $I_{\alpha,\alpha'}(\mathbf{q})$ is the exciton-phonon matrix element equal to

$$I_{\alpha,\alpha'}(q) = \int \Psi_\alpha^* (\mathbf{r}_e, \mathbf{r}_h) \left(e^{i\mathbf{q}\cdot\mathbf{r}_e} - e^{i\mathbf{q}\cdot\mathbf{r}_h} \right) \Psi_{\alpha'} (\mathbf{r}_e, \mathbf{r}_h) \times d^3 r_e d^3 r_h, \tag{11}$$

where $\Psi_\alpha (\mathbf{r}_e, \mathbf{r}_h)$ is the wave function of the α state of the exciton. The solution of $\{G(k_0, E)\}^{-1} = 0$ determines the excitation spectrum of the EHP-phonon system. We are interested in this spectrum for $K' = 0$ and $E(0) = \hbar^2 k_0^2 / 2\mu$. If the EHP energy $E(0)$ is close to resonance, i.e., $E(0) \simeq \hbar\omega_{\text{LO}} - R/n^2$, the resonant terms of the sum over α in Eq. (10) will be those corresponding to transitions between the continuum $E_{\text{ex}} = E_0 + \hbar^2 k_0^2 / 2\mu$ and the discrete spectrum $E_{\text{ex}} = E_0 - R/n^2$. The remaining terms in the sum over α are nonresonant and can be eliminated by slight renormalization at the gap E_0 in Eq. (6). They will be disregarded from now on. In the calculation the matrix element $I_{\alpha,\mathbf{k}_0}(\mathbf{q})$ is evaluated by replacing the EHP wave function in the continuum by the free electron-hole wave function with total momentum $\mathbf{K} = 0$, $\mathbf{k}_0 = \mathbf{k}_e = -\mathbf{k}_h$ and relative coordinate $\boldsymbol{\rho}$, that is

$$\Psi_{\mathbf{k}_0}(\boldsymbol{\rho}) = \frac{e^{i\mathbf{k}_0\cdot\boldsymbol{\rho}}}{\sqrt{V_0}}. \tag{12}$$

To simplify the calculation we take for n only the $1s$ state. The wave function $\Psi_{1s}(\boldsymbol{\rho})$ is then isotropic and we can choose a coordinate system such that the vector $\mathbf{Q} - \mathbf{k}_0$ is parallel to the z axis; in this case we obtain

$$I_{1s,\mathbf{k}_0}(\mathbf{q}) = 8\sqrt{\frac{\pi a^3}{V_0}} [(1 + |\mathbf{t} - \mathbf{Q}_h|^2)^{-2} - (1 + |\mathbf{t} + \mathbf{Q}_e|^2)^{-2}] \delta_{\mathbf{K}+\mathbf{q},0}, \tag{13}$$

where

$$\mathbf{t} = a\mathbf{k}_0, \quad \mathbf{Q}_{e(h)} = \mathbf{Q}\frac{m_{e(h)}}{m_T}, \quad \mathbf{Q} = a\mathbf{q}. \tag{14}$$

Taking Eq. (13) into account, $\Sigma(E, k_0)$ in units of the exciton Rydberg is found to be

$$\frac{\Sigma(E, k_0)}{R} = A_0 \frac{t^2}{\pi} \int_0^\infty \frac{[F(Q,t) + F(-Q,t)] \, dQ}{[E/R - \hbar\omega_{\text{LO}}/R + 1 - (\mu/m_T)Q^2 + i\delta_{1s}/R]}, \tag{15}$$

with

$$F = \frac{1}{6tQ_h} \frac{1}{\left[1 + (t - Q_h)^2\right]^3} + \frac{1}{6tQ_e} \frac{1}{\left[1 + (t - Q_e)^2\right]^3} + \frac{1}{tQ} \frac{1}{1 + t^2 + Q_e Q_h} \frac{1}{\left[1 + (t - Q_h)^2\right] \left[1 + (t + Q_e)^2\right]} - \frac{2Q_h}{tQ^2} \frac{1}{(1 + t^2 + Q_e Q_h)^2} \frac{1}{\left[1 + (t - Q_h)^2\right]} + \frac{2Q_h Q_e}{tQ^3} \frac{1}{(1 + t^2 + Q_e Q_h)^3} \ln \left(\frac{(Q_h - t + i)(Q_e - t + i)}{(Q_h + t + i)(Q_e + t + i)} \right), \tag{16}$$

$$A_0 = \frac{16}{\pi^2} \frac{\hbar\omega_{\text{LO}} e^2}{R^2 a} \left(\epsilon_\infty^{-1} - \epsilon_0^{-1} \right). \tag{17}$$

An analytical expression for $\Sigma(E, k_0)$ can be obtained. Because of its bulkiness, however, we do not present it here. The complete set of parameters needed to evaluate the self-energy by means of Eq. (15) is summarized in Table I. The dimensionless parameter A_0, introduced in Eq. (15), determines the coupling strength between the $1s$-exciton + LO-phonon and EHP states. According to the parameters given in Table I the stronger coupling

TABLE I. Parameters used for the evaluation of luminescence profiles in InP, GaAs, and CdTe.

Parameters	Values InP	GaAs	CdTe
R	5.1 meV[a]	4 meV[d]	10.5 meV[a]
E_0	1421 meV[b]	1506 meV[e]	1606 meV[a]
$\hbar\omega_{\rm LO}$	43 meV[c]	36.7 meV[f]	21 meV[a]
m_e	$0.079m_0$[b]	$0.067m_0$[b]	$0.09m_0$[a]
$m_{\rm hh}$	$0.45m_0$[b]	$0.45m_0$[b]	$0.81m_0$[a]
$m_{\rm lh}$	$0.12m_0$[b]	$0.082m_0$[b]	$0.12m_0$[a]
ε_0	12.61[b]	12.4[a]	10.05[a]
ε_∞	9.61[b]	10.7[a]	7.1[a]

[a] Reference 13.
[b] Reference 12.
[c] Reference 14.
[d] Reference 15.
[e] Reference 16.
[f] Reference 17.

strength corresponds to InP ($A_0 = 8.6$), while for GaAs and CdTe smaller values are obtained, $A_0 = 4.4$ and $A_0 = 2.8$, respectively.

In Fig. 2 the real and imaginary parts of $\Sigma(E, k_0)$ are displayed for InP, GaAs, and CdTe as a function of energy, including only the heavy-hole contribution. Similar analysis performed for the light-hole valence band showed that its contribution to Σ is negligible. Figure 2 shows that for values of $E \gtrsim \hbar\omega_{\rm LO} - R$ the self-energy is a rapidly varying function of the electron-hole pair energy. This means that the exciton continuum couples strongly to the $1s$-exciton state through the LO-phonon field. According to Fig. 2 and Eq. (15) the imaginary part of Σ is negative and presents a minimum for an energy near $\hbar\omega_{\rm LO} - R$, while the real part of $\Sigma \approx 0$ in the same energy range [the reason why this does not happen at $E = \hbar\omega_{\rm LO} - R$ but sligthly above lies in the $\mathbf{K}$ dependence of Eq. (10)]. Consequently, an energy-independent exciton lifetime broadening for the calculation of the annihilation probability W_{cv} would be a bad approximation.

The calculation of Σ has been performed to second order in C_F. In the next higher order, two diagrams appear [see Fig. 1(b)]. They lead to contributions to Σ proportional to $|C_F|^4$, which can be neglected for sufficiently small values of C_F.

C. Spectrum of the EHP-phonon system

To determine the spectrum of the EHP-phonon quasiparticle we calculate the poles of the causal Green's function $G(k_0, E)$ by replacing the self-energy by the approximate expression of $\Sigma(E, k_0)$ given in Eq. (15). The real part of energies $E(k_0)$ calculated for GaAs, InP, and CdTe versus the dimensionless parameter ak_0 are shown in Fig. 3. The error bars correspond to the imaginary part of $E(k_0)$. Note that in Fig. 3(b) of Ref. 1 only the solution of $\mathrm{Re}\{G^{-1}\} = 0$ was plotted. For comparison, the spectrum $E(k_0)$ calculated for InP without electron-phonon interaction is also displayed (dashed line). In these figures the solid lines represent the renormalized spectra of the EHP–LO-phonon system. From Fig. 3 it is clear that the resulting dispersion relations exhibit two branches with energies below and above the unperturbed ones. The calculated energies for GaAs and CdTe display a similar feature which is weaker than that of InP, a fact which reflects the smaller dimensionless coupling parameter A_0. The peculiar behavior observed in the case of CdTe may be due to the fact that the approximation of a free electron-hole continuum used in the calculation [Eq. (12)] is not good for values of $\hbar\omega_{\rm LO}$ which are not large compared to R. For the calculation a Lorentzian broadening $\delta_{1s} = 1$ meV was taken in all cases. With increasing δ_{1s} the EHP-phonon self-energy becomes weaker and soon disappears, thus the conventional unperturbed EHP continuum energy is recovered.[1]

The structure found in the self-energy $\Sigma(E, k_0)$ modifies the spectral function

$$A(k_0, \hbar\omega_l) = -\frac{1}{\pi}\mathrm{Im}G\,(k_0, \hbar\omega_l - E_0)\,, \tag{18}$$

the density of EHP continuum states

$$g(E) = -\frac{1}{\pi}\mathrm{Im}\sum_{\mathbf{k}_0} G(k_0, E), \tag{19}$$

and, consequently, the photon-emission rate. According to Eqs. (6) and (15), the density of states $g(E)$ of the EHP-phonon quasiparticle exhibits a dip at $E = \hbar\omega_{\rm LO} - R$ with respect to that of the unperturbed EHP continuum states $g_0(E) = -\pi^{-1}\mathrm{Im}\sum_{\mathbf{k}_0} G^0(k_0, E)$ (for more details see Ref. 1). These are much weaker for GaAs

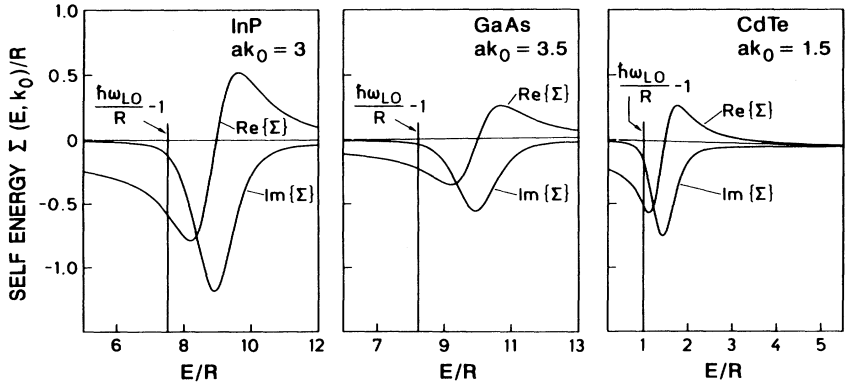

FIG. 2. The resonant part of the self-energy $\Sigma(E, k_0)$ for electron heavy-hole pairs in InP, GaAs, and CdTe with $ak_0 = 3$, 3.5, and 1.5, respectively, and an exciton width $\delta_{1s} = 1$ meV. Both Σ and E are in units of the exciton Rydberg.

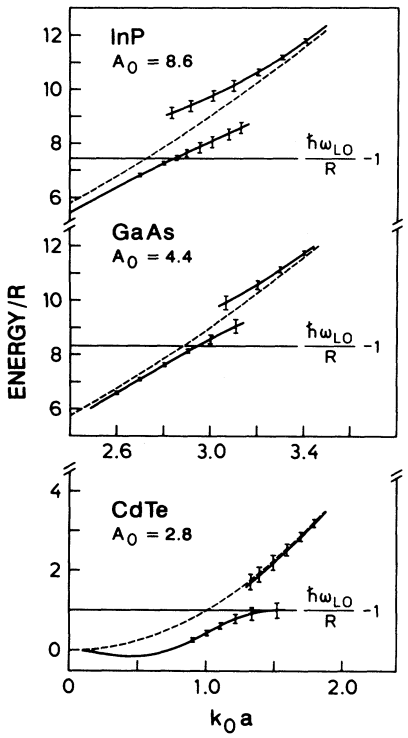

FIG. 3. The calculated spectrum of the real part of $E(k_0)$ for the EHP–LO-phonon system as a function of the EHP relative wave vector $|\mathbf{k}_0|$ for GaAs, InP, and CdTe. The value of $\delta_{1s} = 1$ meV and the parameters for the heavy-hole valence band of Table I were used in the calculation. The energy E is given in units of the exciton Rydberg, $|\mathbf{k}_0|$ in units of inverse exciton Bohr radii a^{-1}. The dashed lines represent the unperturbed EHP continuum energy for InP. The vertical flags represent the imaginary part of $E(k_0)$.

and CdTe than for InP, a fact which reflects the differences in A_0.

III. ELECTRON-HOLE DISTRIBUTION FUNCTION

In order to obtain the photon-emission rate $I_{\rm em}(\hbar\omega_l)$ with Eq. (1), the EHP distribution function $P(\mathbf{k}_e, \mathbf{k}_h)$ must be calculated. The luminescence spectrum of InP above the gap at $T = 5$ K reported in Ref. 1 shows an average thermal distribution with an effective temperature $T_e \simeq 90$ K. This means that the EHP relaxes through phonon emission in a large range of the continuum EHP energy before its recombination. The relevant distribution function corresponds to a nonequilibrium situation and depends on the scattering rate by optic and acoustic phonons down to the bottom of the continuum band. To simplify the calculation, we shall neglect in the following correlations between electrons and holes. This approximation is supported by the fact that the internal energy for EHP in the continuum is of the order of $\hbar\omega_{\rm LO}$, i.e., $\Delta E \sim \hbar\omega_{\rm LO} \gg R$. Consistent with this, we also neglect, as a first-order approximation, the phonon-induced energy renormalization of the continuum energies described above. This renormalization will, however, appear in Eq. (1) through W_{cv} [see Eq. (2)]. Within this approximation the distribution $P(\mathbf{k}_e, \mathbf{k}_h)$ can be written as

$$P(\mathbf{k}_e, \mathbf{k}_h) = P_c(\mathbf{k}_e) P_v(\mathbf{k}_h), \tag{20}$$

where $P_c(\mathbf{k}_e)$ $[P_v(\mathbf{k}_h)]$ represents the electron (hole) distribution function (EDF) in the conduction (valence) band. We assume isotropic parabolic bands.

Assuming phonons in equilibrium at the temperature T the distribution function satisfies a semiclassical *master equation* of the form

$$\frac{\partial P(\mathbf{k}, t)}{\partial t} = W_{\rm in}(\mathbf{k}, t) - W_{\rm out}(\mathbf{k}, t), \tag{21}$$

where $W_{\rm in}$ represents all contributions per unit time to the state with wave vector $\mathbf{k}$, and conversely for $W_{\rm out}$. We may represent $W_{\rm in}$ as

$$W_{\rm in} = \sum_{\mathbf{k}'} P(\mathbf{k}', t) w(\mathbf{k}', \mathbf{k}), \tag{22}$$

$w(\mathbf{k}', \mathbf{k})$ being the transition rate from the $\mathbf{k}'$ to the $\mathbf{k}$ electron state. In $W_{\rm out}$ we include radiative $(1/\tau)$ and nonradiative $(1/\tau_{\rm NR})$ processes represented by the phonon-induced scattering rate $w(\mathbf{k}, \mathbf{k}')$ from $\mathbf{k}$ to $\mathbf{k}'$. We thus write

$$W_{\rm out} = \sum_{\mathbf{k}'} P(\mathbf{k}, t) w(\mathbf{k}, \mathbf{k}') + \frac{P(\mathbf{k}, t)}{\tau}. \tag{23}$$

Using Eqs. (22) and (23) and assuming an isotropic EDF the master equation is transformed to

$$\int w(\varepsilon', \varepsilon) P(\varepsilon') d\varepsilon' - \int w(\varepsilon, \varepsilon') P(\varepsilon) d\varepsilon - \frac{P(\varepsilon)}{\tau} = 0, \tag{24}$$

where now $P(\varepsilon)d\varepsilon$ is the electron density in the energy interval $(\varepsilon, \varepsilon + d\varepsilon)$ and $w(\varepsilon', \varepsilon)$ the electronic transition rate from ε' to ε. In Eq. (24) it is assumed that electrons have reached a configuration stationary in energy.

The exact solution of Eq. (24) for arbitrary energy and temperature is a very difficult task. Nevertheless, for temperatures in the range $k_B T \ll \hbar\omega_{\rm LO}$ LO-phonon absorption is negligible and LO-phonon emission is energetically forbidden for electron energies $\varepsilon < \hbar\omega_{\rm LO}$. In this energy interval electron scattering by LA phonons dominates the relaxation process. Let us first solve Eq. (24) in the energy interval $\varepsilon < \hbar\omega_{\rm LO}$. Using Fermi's golden rule and phonons described by a Debye model one can show that [see Eq. (A8)]

$$w_{ac}(\varepsilon', \varepsilon) = \sqrt{\frac{\varepsilon}{\varepsilon'}} e^{(\varepsilon' - \varepsilon)/k_B T} w_{ac}(\varepsilon, \varepsilon'). \tag{25}$$

Using this relation Eq. (24) can be written as

$$\int w_{ac}(\varepsilon, \varepsilon') \left[f(\varepsilon') - f(\varepsilon) \right] d\varepsilon' - \frac{f(\varepsilon)}{\tau} = 0, \tag{26}$$

where

$$f(\varepsilon) = \frac{e^{\varepsilon/k_B T}}{\sqrt{\varepsilon}} P_{ac}(\varepsilon). \tag{27}$$

Noting that the electron energy is changed only by a small amount (see the Appendix) after LA-phonon absorption or emission, the function $f(\varepsilon')$ can be expanded in a Taylor series about ε,

$$f(\varepsilon') = \sum_{n=0}^{\infty} \frac{(\varepsilon' - \varepsilon)^n}{n'} \frac{d^n f(\varepsilon)}{d\varepsilon^n}. \tag{28}$$

After the substitution of Eq. (28) into Eq. (26) we are able to reduce the master equation to a differential equation for $f(\varepsilon)$. A simpler appproximate equation is obtained by retaining terms up to first order in n. The resulting first-order differential equation is

$$a_1(\varepsilon)\frac{df}{d\varepsilon} - \frac{f}{\tau} = 0 \tag{29}$$

with

$$a_1(\varepsilon) = \int (\varepsilon' - \varepsilon) w(\varepsilon', \varepsilon) d\varepsilon. \tag{30}$$

In the Appendix a calculation of $a_1(\varepsilon)$ in the limit $k_B T \gg 2mu^2$ is performed for deformation-potential scattering. Using the relation (A9) for $a_1(\varepsilon)$ and after substitution in Eq. (29) we obtain the distribution function given by

$$P_{ac}(\varepsilon) = N_0 \sqrt{\varepsilon} e^{-\varepsilon/k_B T_e}, \quad \varepsilon < \hbar\omega_{\mathrm{LO}} \tag{31}$$

where T_e is an effective temperature equal to

$$\frac{1}{k_B T_e} = \frac{1}{k_B T} - \frac{\tau_{ac}(\varepsilon, T)}{4mu^2 \tau} \tag{32}$$

and N_0 a normalization factor.

Thus, for $\varepsilon < \hbar\omega_{\mathrm{LO}}$ the luminescence process is described by the EDF given by Eq. (31) which is conditioned by two lifetimes, the relaxation time τ_{ac} and the nonphonon relaxation τ. If $\tau_{ac} \gg \tau$ a strong nonequilibrium EDF is obtained with an effective temperature T_e higher than the crystal temperature T. If $\tau \gg \tau_{ac}$ a thermal quasiequilibrium electron sets on, leading to thermalized luminescence with $T_e \simeq T$ and the EDF given by Eq. (31) reduces to a Maxwell-Boltzmann one.

Let us analyze the case $\varepsilon \gtrsim \hbar\omega_{\mathrm{LO}}$. In this case the emission of LO phonons by the electrons is not forbidden and the transition rate $w(\varepsilon, \varepsilon')$ is affected by the electron–LO-phonon Fröhlich Hamiltonian. Then, for $k_B T \ll \hbar\omega_{\mathrm{LO}}$ we have

$$w(\varepsilon, \varepsilon') = w_{ac}(\varepsilon, \varepsilon') + \frac{1}{\tau_{\mathrm{LO}}(\varepsilon)} \delta(\varepsilon - \varepsilon' - \hbar\omega_{\mathrm{LO}}). \tag{33}$$

In Eq. (33) τ_{LO}^{-1} is the LO-phonon emission rate at zero temperature,[19]

$$\frac{1}{\tau_{\mathrm{LO}}(\varepsilon)} = 2\alpha\omega_{\mathrm{LO}} \left(\frac{\hbar\omega_{\mathrm{LO}}}{\varepsilon}\right)^{1/2} \times \ln \left| \left(\frac{\varepsilon}{\hbar\omega_{\mathrm{LO}}}\right)^{1/2} + \left(\frac{\varepsilon}{\hbar\omega_{\mathrm{LO}}} - 1\right)^{1/2} \right| \tag{34}$$

for $\varepsilon \geq \hbar\omega_{\mathrm{LO}}$,

$$\alpha = \frac{e^2}{2\hbar\omega_{\mathrm{LO}}} \left(\varepsilon_\infty^{-1} - \varepsilon_0^{-1}\right) \left(\frac{2m\omega_{\mathrm{LO}}}{\hbar}\right)^{1/2}, \tag{35}$$

ε_0 and ε_∞ being the static and high-frequency dielectric constant, respectively.

Substituting Eqs. (33) and (34) into Eq. (24) we obtain

$$\gamma(\varepsilon) P(\varepsilon) = \int w_{ac}(\varepsilon', \varepsilon) P(\varepsilon') d\varepsilon' + \frac{P(\varepsilon + \hbar\omega_{\mathrm{LO}})}{\tau_{\mathrm{LO}}(\varepsilon + \hbar\omega_{\mathrm{LO}})}, \tag{36}$$

where $\gamma(\varepsilon)$ is the inverse lifetime of the electron given by

$$\gamma(\varepsilon) = \frac{1}{\tau_{ac}(\varepsilon)} + \frac{1}{\tau_{\mathrm{LO}}(\varepsilon)} + \frac{1}{\tau}. \tag{37}$$

The solution of the integral equation (36) can be obtained by an iteration procedure in such a way that[20]

$$P(\varepsilon) = \lim_{j \to \infty} \{P^{(j)}(\varepsilon)\}, \tag{38}$$

where $P^{(j)}(\varepsilon)$ satisfies the following recurrence relation:

$$\gamma(\varepsilon) P^{(j)}(\varepsilon) = \int w_{ac}(\varepsilon', \varepsilon) P^{(j-1)}(\varepsilon) d\varepsilon' + \frac{P^{(j-1)}(\varepsilon + \hbar\omega_{\mathrm{LO}})}{\tau_{\mathrm{LO}}(\varepsilon + \hbar\omega_{\mathrm{LO}})}, \quad j = 1, 2, \ldots . \tag{39}$$

As $j = 0$ function we take $P^{(0)}(\varepsilon) = P_{ac}(\varepsilon)$ given by Eq. (31), thus, to first order, it follows from Eq. (39) that

$$P^{(1)}(\varepsilon) = N_0 \sqrt{\varepsilon} e^{-\varepsilon/k_B T_e} \left(1 + \frac{\tau_{ac}(\varepsilon)}{\tau_{\mathrm{LO}}(\varepsilon)} + \frac{\tau_{ac}(\varepsilon)}{\tau}\right)^{-1} + \frac{P_{ac}(\varepsilon + \hbar\omega_{\mathrm{LO}})}{\tau_{\mathrm{LO}}(\varepsilon + \hbar\omega_{\mathrm{LO}})}, \quad \varepsilon > \hbar\omega_{\mathrm{LO}}. \tag{40}$$

From the structure of Eqs. (39) and (40) it can be seen that $P^{(j)}(\varepsilon)$ $(j \geq 2)$ contains terms of the type $\left(\frac{\tau_{\mathrm{LO}}}{\tau_{ac}}\right)^j$, thus, and because we deal with an energy range $\varepsilon < 2\hbar\omega_{\mathrm{LO}}$, iterations in $P(\varepsilon)$ with $j \geq 2$ need not be considered since $\tau_{\mathrm{LO}} \ll \tau_{ac}$. For the III-V and II-VI semiconductors electron coupling with a LO phonon is dominant since it is allowed by energy conservation. The relaxation time due to phonon scattering can be estimated as follows: $\tau_{ac} \simeq 10^{-12}$ s for LA phonons, while $\tau_{\mathrm{LO}} \simeq 10^{-13}$ s for LO phonons (see Refs. 21 and 22), and indeed τ_{ac} is much larger than τ_{LO}. By comparing Eqs. (31) and (40) it is clear that the electron distribution in energy is drastically reduced for electron kinetic energies ε larger than $\hbar\omega_{\mathrm{LO}}$. Moreover, the electron recombination time τ is of the order of 10^{-10} s, i.e., much larger than the relaxation time due to phonons. The radiative recombination is therefore a rather slow process compared with the scattering process τ_{ac}. In solving Eq. (24) electron relaxation τ_i^{-1} due to electron-impurity interaction has been neglected. An estimation of τ_i for the impurity concentration N_i can be obtained with the Conwell-Weisskopf formula[23]

$$\tau_i \approx \frac{\sqrt{2m}\varepsilon_0^2}{\pi e^4 N_i} \varepsilon^{3/2}. \tag{41}$$

The electron-impurity interaction can be neglected if $\tau_i \gg \tau_{ac}$. From Eqs. (41) and (A10) (see the Appendix) it follows that this is the case for

$$N_i \ll \left[\frac{\varepsilon_0 C_0 m}{\pi e^2 \hbar^2 u}\right]^2 \frac{k_B T}{\rho}\varepsilon^2. \tag{42}$$

Using typical parameters for InP, with $\varepsilon \sim \hbar\omega_{\rm LO}$ in (42), we find $N_i < 5 \times 10^{15}$ cm^{-3} for $T = 5$ K and $N_i < 2 \times 10^{16}$ cm^{-3} for $T = 30$ K. In Ref. 1 the experiments were performed for an InP sample with $N_i = 3 \times 10^{13}$ cm^{-3}. The corresponding expression for the hole distribution function (DF) can be easily obtained from Eqs. (31) and (40), replacing the electron parameters by the appropriate hole parameters.

For the hole valence bands it is possible to define appropriate effective deformation potentials $C_{\rm eff}$ which include all of the complications of the valence bands.[24] In the acoustic mode case $C_{\rm eff}$ is given by[25]

$$C_{\rm eff}^2 = a^2 + \frac{c_l}{c_t}\left(b^2 + \frac{1}{2}d^2\right), \tag{43}$$

where a, b, and d are the fundamental valence-band deformation potentials and c_l and c_t the spherically averaged elastic compliance constants. The velocity u is, in this case, an average sound velocity given by $u^2 = \frac{1}{3}u_l^2 + \frac{2}{3}u_t^2$, where u_l and u_t are the longitudinal and transverse sound-wave velocities, respectively.

IV. LUMINESCENCE INTENSITY

Taking into consideration Eqs. (1) and (7) it follows that

$$I_{\rm em}(\hbar\omega_l) = -\Lambda\,{\rm Im}\left\{\int \frac{e^{\pi\sqrt{R/\varepsilon}}}{\sinh\left(\sqrt{R/\varepsilon}\right)} P_e\left(\frac{\mu}{m_e}\varepsilon\right) P_h\left(\frac{\mu}{m_h}\epsilon\right)\left[\hbar\omega_l - E_0 - \varepsilon - \Sigma(\hbar\omega_l - E_0, \varepsilon) - i\delta_0\right]^{-1} d\varepsilon\right\}, \tag{44}$$

where

$$\Lambda = \frac{4R\,|\hat{\varepsilon}\cdot\mathbf{p}_{cv}|^2}{\hbar^2\omega_l m_0 n}\left(\frac{\mu}{m_0}\right)^{3/2}. \tag{45}$$

Substituting the DF given by Eqs. (31) and (40) for the electrons and holes in Eq. (44) the luminescence intensity $I_{\rm em}(\hbar\omega_l)$ above the gap has been calculated for InP [see Fig. 4(a)] at different effective temperatures. Figure 4(a) shows how the optical emission tail decreases with decreasing T_e. Moreover, near the emitted photon energy $\hbar\omega_l \sim E_0 - \hbar\omega_{\rm LO}$ a nonmonotonic structure modifies the exponential tail. Here, the calculated emission spectra reflects the changes of the electron-hole distribution energy, the spectrum of the EHP–LO-phonon quasiparticle, and its resonant behavior for $\hbar\omega_l \approx E_0 - R + \hbar\omega_{\rm LO}$ through the imaginary part of Σ. By comparison, the calculated intensities without electron–LO-phonon interaction (dashed lines) are presented for the same effective temperatures. In this case the DF is described only by Eq. (31) on the whole range of electron kinetic energy; that is, the relaxation time is determined by acoustic phonons. Thus no structure is observed modifiying the standard optical emission tail.

Figure 4(b) shows calculations for GaAs and CdTe with $T_e = 90$ K. Besides the parameters listed in Table I, the ratio $\tau_{ac}/\tau_{\rm LO} = 50$ and the $1s$ exciton with $\delta_{1s} = 1$ meV were used for these calculations. These figures show only changes in the emission tail related to the effect of the LO phonons on the DF for $\hbar\omega_l \gtrsim E_0 - R + \hbar\omega_{\rm LO}$. The fact that no features related to self-energy effects appear is explained by the small values of the coupling strength parameter A_0 [see Eq. (17)] which produce a

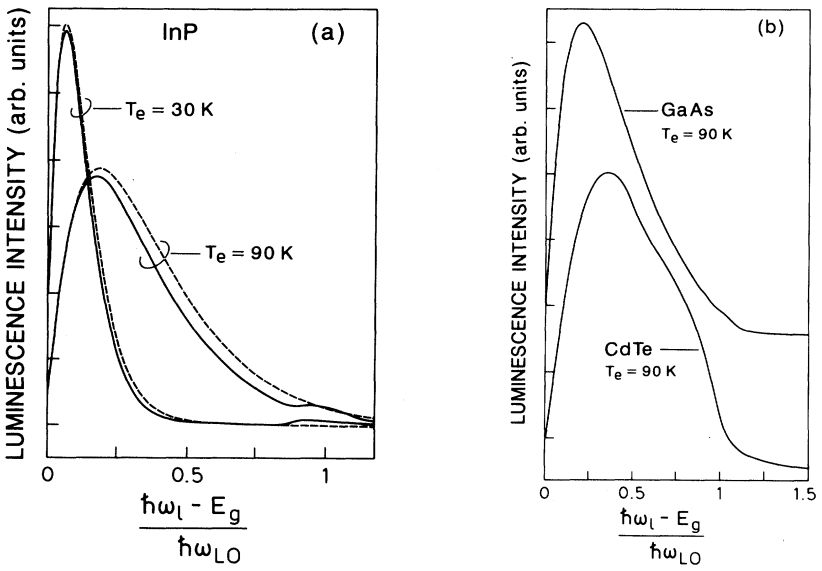

FIG. 4. (a) Luminescence spectra of InP (solid lines) calculated according to Eq. (44) for two different effective temperatures T_e = 30 and 90 K. The dashed lines correspond to the same calculation neglecting the electron–LO-phonon interaction. (b) Luminescence spectrum calculated for GaAs and CdTe semiconductors according to Eq. (44) with an effective temperature $T_e = 90$ K. The curves are shifted vertically for clarity.

weak structure in the spectrum of the EHP-phonon system (see Fig. 3) and a very weak dip in the density of states $g(\varepsilon)$. As mentioned in Sec. II C the results for CdTe are not expected to be very reliable because of the inaccuracy involved in the uncorrelated continuum approximation. The structure calculated at $\hbar\omega_l - E_q \simeq \hbar\omega_{\rm LO}$ for GaAs is considerably weaker than that found for InP, this being due to the smaller value of A_0. The ability to observe this structure is determined by noise in the experimental data (one would have lower noise than in Fig. 5 in order to make the structure observable for GaAs) and also by the total width of the exciton ground state determined by electron decay channels, not considered here, plus inhomogeneous broadening.

Figure 5 depicts the luminescence profile measured for InP above the gap at $T \lesssim 5$ K (Ref. 1) together with the $I_{\rm em}(\hbar\omega_l)$ calculated with Eq. (44). An effective temperature $T_e = 90$ K was used in the calculation, which corresponds to an electron lifetime $\tau_{ac} = 0.05\,\tau$ for a crystal temperature $T = 5$ K. The theoretical curve reproduces well the main features of the luminescence profile. In Fig. 6 we compare our calculation with the experimental results for InP at different crystal temperatures ($T = 5$, 22, and 27 K). The variation with T follows from the dependence of the effective temperature T_e on T [Eq. (32)]. In the whole temperature range considered here we took $\tau_{ac}/\tau_{\rm LO} = 50$ for $\hbar\omega_l > E_0 - R + \hbar\omega_{\rm LO}$ and $\delta_{1s} = 0.8$ meV.[13] The dip we observe in Fig. 6 at $\hbar\omega_l$ around 1.460 eV is due in our calculation to the resonant reduction in the excitonic component of the mixed exciton-phonon system, i.e., to the resonant behavior of the self-energy at $\hbar\omega_l \approx E_0 - R + \hbar\omega_{\rm LO}$. The maximum at $\hbar\omega_l$ near 1.463 eV corresponds to the bottleneck in the optical emission, according to Eq. (40). For electron or hole kinetic energies higher than $\hbar\omega_{\rm LO}$, the scattering by LO phonons is switched on and the distribution of electrons (holes) in energy is drastically reduced.

V. CONCLUSIONS

We have developed a theoretical model of phonon side bands in optical emission which describes the luminescence profile above the gap in zinc-blende-type semiconductors. We show that a resonant structure in the electron-hole pair continuum results from the interaction with the $1s$ exciton plus one LO-phonon complex. The resonant exciton-phonon quasiparticle spectrum is governed by the dimensionless parameter A_0 given by Eq. (17) and the effective reduced mass. A higher value of A_0 produces a strong-coupling strength of the EHP–LO-phonon system which modifies substantially the spectral function and the density of EHP states around the energy $E \approx \hbar\omega_{\rm LO} - R$. The electron-hole nonequilibrium distribution function so obtained depends on an effective

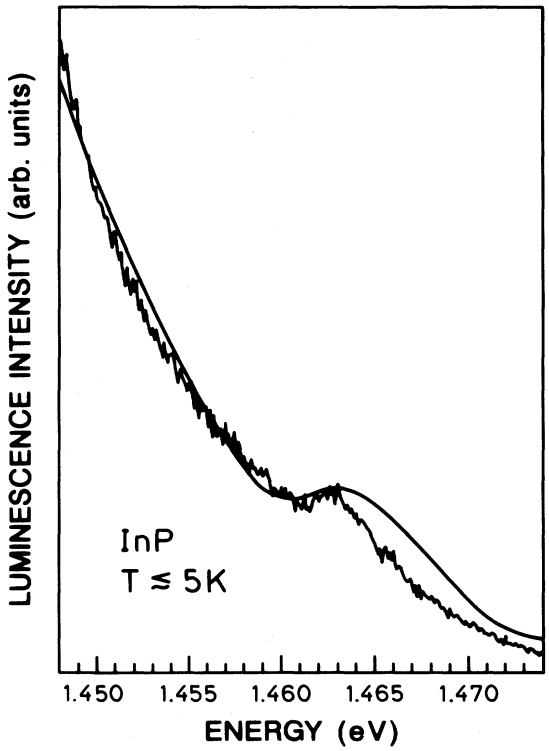

FIG. 5. Luminescence spectrum of InP above the gap for $T \lesssim 5$ K (Ref. 1). The solid line represents the calculated profile performed, according to Eq. (44), for electron–heavy-hole pairs.

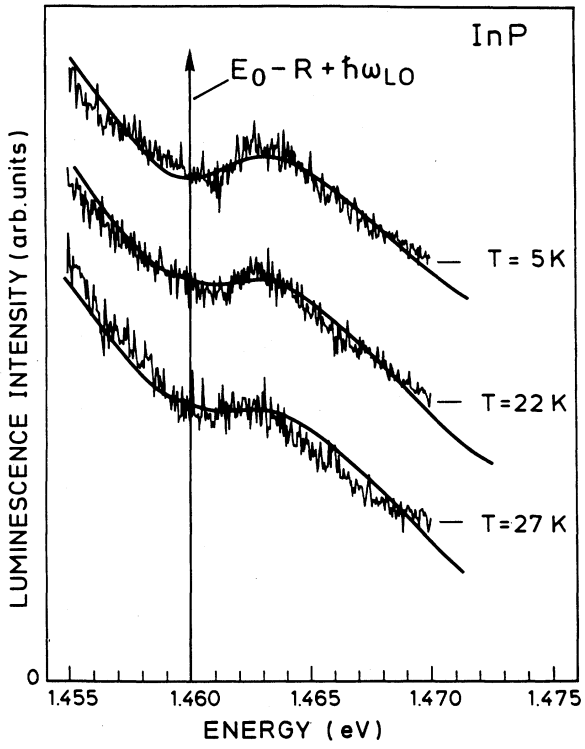

FIG. 6. Luminescence profile of InP taken at different crystal temperatures and for emitted photon energies near $E_0 - R + \hbar\omega_{\rm LO}$ (Ref. 1). The solid lines correspond to luminescence profiles calculated using Eq. (44) and Eq. (32) including the dependence on crystal temperature.

temperature which involves the ratio of the acoustical relaxation time and the radiative recombination time. The calculated luminescence profile agrees rather well with experimental data for InP, giving support to the idea that the observed structure of Ref. 1 arises from the recombination of resonant exciton-phonon quasiparticles. The failure to observe such a structure in GaAs and CdTe is explained, in the framework of our theoretical model, by the smaller electron-phonon coupling constant.

ACKNOWLEDGMENTS

C.T.-G. wishes to thank the Max-Planck-Institut für Festkörperforschung for the hospitality. F.I. thanks the Alexander von Humboldt-Foundation and the Conselho Nacional de Pesquisa for financial support. Thanks are also due to V.I. Belitsky for a critical reading of the manuscript.

APPENDIX A: SCATTERING PROBABILITY $w(\varepsilon, \varepsilon')$

We consider electron scattering by LA phonons with the dispersion law $w_q = uq$, u being the sound velocity and $\mathbf{q}$ the phonon wave vector. The probability $w(\varepsilon, \varepsilon')$ can be easily obtained using Fermi's golden rule,

$$W_{ac}(\varepsilon) = \frac{2\pi}{\hbar} \sum_f |\langle f | H_{e\text{-}p} | i \rangle|^2 \delta(\varepsilon_i - \varepsilon_f), \tag{A1}$$

where ε_i (ε_f) represents the initial (final) energy of the system. The electron–LA-phonon Hamiltonian for the deformation-potential model is

$$H_{e\text{-}p} = \sum_{\mathbf{q}} \left(c_{\mathbf{q}} e^{i\mathbf{q}\cdot\mathbf{r}} b_{\mathbf{q}} + c^*_{\mathbf{q}} e^{-i\mathbf{q}\cdot\mathbf{r}} b^+_{\mathbf{q}} \right), \tag{A2}$$

where $b_{\mathbf{q}}$ ($b^+_{\mathbf{q}}$) is the annihilation (creation) operator of the LA-acoustic phonon, and

$$c_{\mathbf{q}} = \left(\frac{\hbar}{2V_0 \rho_0 u} \right)^{1/2} q^{1/2} C_0, \tag{A3}$$

ρ_0 is the crystal density and C_0 the electron or hole deformation potential. Using Eqs. (A1)–(A3) the transition probability becomes equal to

$$W_{ac}(\varepsilon) = \frac{D}{\sqrt{\varepsilon}} \left\{ \int_{\varepsilon}^{\varepsilon_+} (\varepsilon' - \varepsilon)^2 N\left(\frac{\varepsilon' - \varepsilon}{k_B T} \right) d\varepsilon' + \int_{\varepsilon_-}^{\varepsilon} (\varepsilon - \varepsilon')^2 \left[1 + N\left(\frac{\varepsilon - \varepsilon'}{k_B T} \right) \right] d\varepsilon' \right\}, \tag{A4}$$

with

$$D = \frac{C_0^2}{4\pi \rho_0 u^4 \hbar^4} \sqrt{\frac{m}{2}}, \tag{A5}$$

$$N(z) = [\exp(z) - 1]^{-1}, \tag{A6}$$

$$\varepsilon_\pm = \left(\sqrt{\varepsilon} \pm \sqrt{2mu^2} \right)^2. \tag{A7}$$

Thus the scattering probability per unit time and energy is given by

$$w_{ac}(\varepsilon, \varepsilon') = \begin{cases} \frac{D}{\sqrt{\varepsilon}} (\varepsilon' - \varepsilon)^2 N\left(\frac{\varepsilon' - \varepsilon}{k_B T} \right), & \varepsilon \le \varepsilon' \le \varepsilon_+ \\ \frac{D}{\sqrt{\varepsilon}} (\varepsilon - \varepsilon')^2 \left[N\left(\frac{\varepsilon - \varepsilon'}{k_B T} \right) + 1 \right], & \varepsilon_- \le \varepsilon' \le \varepsilon. \end{cases} \tag{A8}$$

From (A8) Eq. (25) is easily derived. Under the approximation $N(\varepsilon/k_B T) \simeq \frac{k_B T}{\varepsilon}$ with $k_B T \gg 2mu^2$, the coefficient $a_1(\varepsilon)$ of Eq. (30) can be evaluated analytically to be

$$a_1(\varepsilon) = \frac{8mu^2}{\tau_{ac}(\varepsilon, T)}, \tag{A9}$$

where τ_{ac} is the electron lifetime equal to[18]

$$\frac{1}{\tau_{ac}} = 8D k_B T m u^2 \sqrt{\varepsilon}. \tag{A10}$$

*On leave from Department of Theoretical Physics, Havana University, Havana, Cuba.

[1] F. Iikawa, C. Trallero-Giner, and M. Cardona, Solid State Commun. **79**, 131 (1991).
[2] Y. Toyozawa and J. Hermanson, Phys. Rev. Lett. **21**, 1637 (1968).
[3] W.Y. Liang and D.A. Yoffe, Phys. Rev. Lett. **20**, 59 (1968).
[4] W.C. Walker, D.M. Roessler, and E. Loh, Phys. Rev. Lett. **20**, 847 (1968).
[5] K. Sak, Phys. Rev. Lett. **25**, 1654 (1970).
[6] H. Been and E.W. Williams, in *Semiconductors and Semimetals*, edited by R.K. Willardson and A.C. Beer (Academic, New York, 1972), Vol. 8, p. 182.
[7] R.J. Elliott, Phys. Rev. **108**, 1384 (1957).

[8]L.I. Korovin and S.T. Pavlov, Zh. Eksp. Teor. Fiz. **53**, 1708 (1967) [Sov. Phys. JETP **26**, 979 (1968)].
[9]A.A. Abrikosov, L.P. Gorkov, and L.Y. Dzyaloshinski, *Quantum Field Theoretical Methods in Statistical Physics* (Pergamon, London, 1965).
[10]R. Kubo, J. Phys. Soc. Jpn. **12**, 570 (1957).
[11]H. Fröhlich, Adv. Phys. **3**, 325 (1954).
[12]*Landolt-Börnstein Tables*, edited by O. Madelung, M. Schulz, and H. Weiss (Springer-Verlag, Berlin, 1982), Vol. 17a.
[13]*Landolt-Börnstein Tables*, edited by O. Madelung, M. Schulz, and H. Weiss (Springer-Verlag, Berlin, 1987), Vol. 22a.
[14]W. Kauschke and M. Cardona, Phys. Rev. B **33**, 5473 (1986).
[15]D.D. Sell, Phys. Rev. B **6**, 3750 (1972).
[16]A.K. Sood, W. Kauschke, J. Menéndez, and M. Cardona, Phys. Rev. B **35**, 2886 (1987).
[17]J. Menéndez and M. Cardona, Phys. Rev. B **31**, 3696 (1985).
[18]J. Bardeen and W. Schockley, Phys. Rev. **80**, 72 (1950).
[19]R.P. Feynman, *Statistical Mechanics* (Benjamin, New York, 1972).
[20]P.M. Morse and H. Feshbach, *Methods of Theoretical Physics* (McGraw-Hill, New York, 1953).
[21]H. Alzmüller, F. Fröschl, and U. Schröder, Phys. Rev. B **19**, 3118 (1979).
[22]G. Beniand and T. Rice, Phys. Rev. B **18**, 768 (1978).
[23]W. Schockley, *Electron and Holes in Semiconductors* (Van Nostrand, New York, 1963).
[24]J.D. Wiley, in *Semiconductor and Semimetals*, edited by R.K. Willardson and A.C. Beer (Academic, New York, 1975), Vol. 10, p. 91.
[25]P. Lawaetz, Phys. Rev. **183**, 730 (1969).